J. Fluid Mech. (1977), *vol.* 81, *part* 2, *pp.* 341–351
Printed in Great Britain

Laboratory models of sea straits

By DAVID A. ANATI, GAD ASSAF
AND RORY O. R. Y. THOMPSON†
The Weizmann Institute of Science, Rehovot, Israel

(Received 30 April 1976)

Two basins maintained at different densities are connected by a relatively shallow strait. If the strait is short, the flow is such that the Froude number is unity. The thickness of the intermediate layer, between the outflow and the inflow, is controlled by the requirement that the Richardson number be critical; this thickness is always about one-fifth of the total depth, both in these experiments and in the Strait of Gibraltar. If the strait is long, the Froude number is less than unity in the interior but increases to unity at each end. A strait may be considered short when its length is less than a few hundred times the sill depth.

1. Short-strait theory

Stommel & Farmer (1953) gave a seminal theory of a two-layer flow for estuaries with a short and narrow opening to the sea. Their basic idea was that the velocities would not increase beyond the point at which long interfacial waves become stationary and that the interfacial Froude number would be unity, i.e.

$$F = U_1^2/g'D_1 + U_2^2/g'D_2 = 1, \tag{1.1}$$

where $g' = g(\rho_2 - \rho_1)/\rho$, U is the mean velocity, D is the flow depth, a subscript 1 refers to the upper layer and a subscript 2 to the lower layer.

Equation (1.1) can be derived in several ways. In our context, we shall examine the steady, linearized, long-wave interface response to small bumps of height h on the bottom. Denote the interface deviation by η. The velocity perturbation is then

$$u_1 = U_1\eta/D_1, \quad u_2 = U_2(h-\eta)/D_2. \tag{1.2), (1.3}$$

Substitution of (1.2) and (1.3) into

$$Uu_x = \rho^{-1}P_x \tag{1.4}$$

gives

$$P_{1x} = -\rho_1 U_1^2\eta_x/D_1, \quad P_{2x} = -\rho_2 U_2^2(h-\eta)_x/D_2, \tag{1.5), (1.6}$$

but

$$P_{2x} = P_{1x} + g\Delta\rho\eta_x \tag{1.7}$$

and therefore

$$[\rho_1 U_1^2/D_1 + \rho_2 U_2^2/D_2 - g\Delta\rho]\,\eta = h\rho_2 U_2^2/D_2. \tag{1.8}$$

As the coefficient of η approaches zero, even very small bumps can cause large interface deviations. Therefore, as the Froude number (1.1) approaches unity, large interfacial waves can be expected, which will choke the flow.

As a model of a short strait, we consider simply a rectangular opening of depth D and width B in a wall separating two boxes with a density difference $\Delta\rho$. We shall consider a source of buoyancy (a heater) that causes only small density differences and conserves

† Present address: CSIRO, Division of Atmospheric Physics, Mordialloc, Victoria, Australia.

mass, and can thus assume that the same flux $Q = U_1 D_1 B = U_2 D_2 B$ flows in each direction. This flux Q is maximized subject to (1.1) for $D_1 = D_2 = \frac{1}{2}D$, so that

$$U_1^2 = U_2^2 = \tfrac{1}{4} g D \Delta\rho/\rho.$$

In the experiments, the density difference is caused by heating one box and cooling the other at a rate H. In a steady state this H must equal the heat flux carried through the strait:

$$H = \tfrac{1}{2}\rho U D B C_p \Delta T, \tag{1.9}$$

where $C_p = 1$ cal/cm^3 °C. Substituting for U and $\Delta\rho = \rho\alpha\Delta T$ in (1.9), the temperature difference ΔT for a given H, subject to the Froude constraint (1.1), is

$$\Delta T = (2/D)\,[2H^2/\alpha g(\rho C_p B)^2]^{\frac{1}{3}}. \tag{1.10}$$

At the interface between the two layers, a shear develops. If this is too sharp, instability to short waves is expected, and the consequent mixing will tend to reduce the shear. This will continue until an equilibrium point is reached, when the Richardson number attains its equilibrium value

$$Ri = -g(\partial\rho/\partial z)/\rho(\partial U/\partial z)^2 = Ri_{\mathrm{eq}}.$$

In a stratified laminar flow, the traditional $Ri_c = \frac{1}{4}$ is expected. In these experiments, however, we have thermal convection in both basins, and wind stress on the cold basin. The fluid entering the constriction is therefore turbulent. The Reynolds number is not large, so viscosity may tend to limit the intensity of the turbulence. There is evidence (e.g. Mellor 1973; Businger *et al.* 1971; Webb 1970) that in the lower atmosphere turbulence decays for

$$Ri > \tfrac{1}{5}. \tag{1.11}$$

We define an interlayer 'thermocline' thickness as $l = \Delta\rho/(\partial\rho/\partial z)_{\max}$. Since turbulent (rather than molecular) processes are considered, we expect (and find below) this thickness to be much the same as $l_u = \Delta U/(\partial U/\partial z)_{\max}$. Therefore $Ri = g\Delta\rho l/\rho\Delta U^2$ and we solve for l, using (1.1) and (1.11):

$$l/D = Ri\,F \sim \tfrac{1}{5}. \tag{1.12}$$

The combination of Froude and Richardson number restrictions leads therefore to the rather curious prediction that the 'thermocline' thickness in a short strait will always be about one-fifth of the total depth, independent of fluxes, geometry, or the properties of the basin.

The above argument does not depend on whether the stratification is due to temperature or salinity. It does depend on the strait being short enough to justify neglecting the bottom friction $C_D U^2/D$ compared with the acceleration uu_x. Thus a strait is short if its length L satisfies

$$L \ll D/C_D. \tag{1.13}$$

Since drag coefficients C_D are usually taken to be $O(10^{-3})$, a strait may be considered short if its length is much less than a thousand times the sill depth.

2. Long-strait theory

For a long strait ($L \gg D/C_D$), inertial forces can be neglected compared with bottom friction. We shall also neglect friction between the layers because we expect the Froude number to drop below critical in the interior of the strait. Therefore the baro-

tropic drop in pressure in the upper layer (which only accelerates the fluid) is negligible compared with the baroclinic drop in pressure in the lower layer (which balances friction). Since the average depth of the lower layer is $\frac{1}{2}D$, the momentum balance is

$$\tfrac{1}{2}g\Delta\rho Dd = \rho C_D \int_0^L U^2 dx. \tag{2.1}$$

Here d is the change in the depth of the interface from one end of the strait to the other. The depth of the lower layer is $\frac{1}{2}(D+d)$ at one end and $\frac{1}{2}(D-d)$ at the other. The velocity $U(x)$ in (2.1) depends on the depth. For simplicity, we shall assume that the depth $D_2(x)$ of the lower layer is linear in x. With $U(x) = Q_2/D_2(x)$, we have

$$\tfrac{1}{2}g'Dd = 4C_D L Q_2^2/(D^2-d^2). \tag{2.2}$$

We require (i) that the same flux Q per unit width flows in each direction and (ii) that relation (1.1) holds at each end of the strait. This Froude condition at each end becomes

$$8Q^2/g'[(D-d)^{-3}+(D+d)^{-3}] = 1. \tag{2.3}$$

Substituting $\gamma = C_D L/2D$ and $\beta = d/D$, and eliminating $Q^2/g'D^3$ between (2.2) and (2.3), we find

$$\beta(1+3\beta^2) = \gamma(1-\beta^2)^2. \tag{2.4}$$

Neglecting terms of order β^2 would yield the convenient result that $\beta = \gamma$, or

$$d/L = \tfrac{1}{2}C_D. \tag{2.5}$$

This is an inclination of the interface of the order of 10^{-3}, which is the value reported by Defant (1961). Equation (2.5) may be applicable to straits of intermediate length, but for long straits the interface comes close to the surface, and terms of order β^2 cannot be neglected. For $\gamma = 1{\cdot}56$, (2.4) gives $\beta = 0{\cdot}5$, in good agreement with the results of Assaf & Hecht (1974). As $\gamma \to \infty$ (very long straits), $\beta \to 1-\gamma^{-\frac{1}{2}}+\frac{3}{4}\gamma^{-1}$ and the flux $Q \to \frac{1}{2}D(\frac{1}{2}g'D)^{\frac{1}{2}}\gamma^{-\frac{3}{4}}$, so less fluid will pass through a longer strait. The Froude number will drop considerably in the interior of a long strait, being already $0{\cdot}19$ for $\gamma = 2$.

If we assume, as before, that the interlayer thermocline thickness l is determined by a critical Richardson number, its fraction of the whole depth, in the interior, is

$$l/D \sim Ri\,F; \tag{2.6}$$

consequently, as the Froude number decreases, the thermocline is expected to sharpen, being already 4 % of the depth for $\gamma = 2$.

A laboratory model with a length several thousands times greater than the depth, and with a large Reynolds number, is rather unrealistic. Instead, a model with laminar side friction rather than turbulent bottom friction is used. Since the reasoning is similar, the results will be relevant. The drag on each layer is now $12\rho\nu QL/B$, and is balanced by pressure gradients. The surface displacement η and the (barotropic) pressure difference $-g\rho\eta$ in the upper layer can no longer be neglected. Assuming symmetry between the upper and lower layer, i.e. $2\eta\rho = d\Delta\rho$, the momentum balance in each layer is

$$12\nu QL/B = \tfrac{1}{2}(\tfrac{1}{2}g'd)\,BD. \tag{2.7}$$

Writing $f = (1-\beta^2)^3/2\beta(1+3\beta^2)$, (2.3) can be rewritten as

$$8Q^2/g'D^3 = \beta f; \tag{2.8}$$

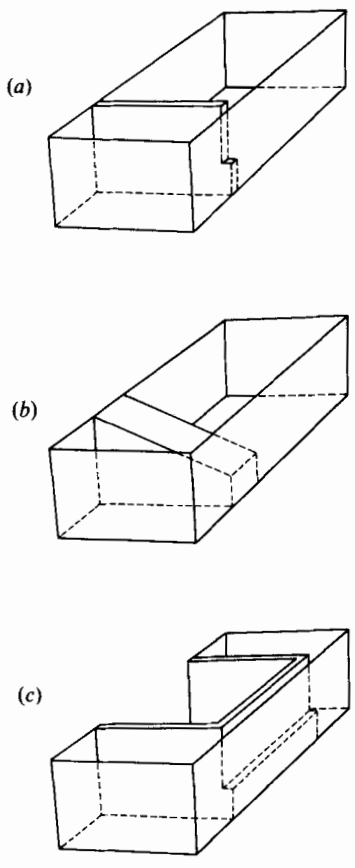

FIGURE 1. Shapes of strait-like constrictions used in the experiments. (*a*) Short rectangular strait. (*b*) Short triangular strait. (*c*) Long rectangular strait.

(2.7) and (2.8) can then be solved for the velocity scale,

$$2Q/D = 12\nu Lf/B^2, \tag{2.9}$$

and the temperature difference (1.9),

$$\Delta T = HB/(6\rho C_p \nu LDf), \tag{2.10}$$

where the interface inclination β must be found from the expression

$$\beta = \frac{6\nu L}{B}\left(\frac{2\rho C_p}{B^2 g\alpha H}\right)^{\frac{1}{3}} \frac{(1-\beta^2)^2}{(1+3\beta^2)^{\frac{2}{3}}}. \tag{2.11}$$

3. Short-strait experiments

A Perspex tank 16 cm wide and 19 cm high was divided by a plate into two basins: one 24 cm long and the other 71 cm long (figure 1*a*). A strait 1·2 cm wide was cut to mid-depth (along one wall, rather than in the centre, to facilitate photography). The tank was filled with water to a height D (= 7 cm unless otherwise specified) above the sill. The small basin was heated (at the bottom, to cause mixing) at a constant rate H by an electric heater. The large basin was cooled by a fan. The top of the heated basin

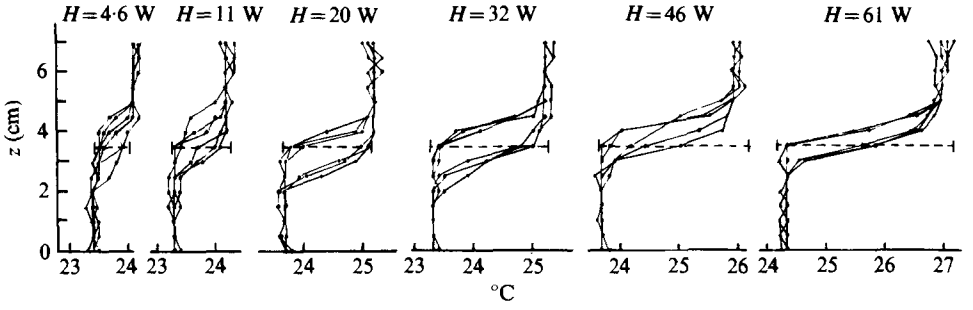

FIGURE 3. Temperature profiles in the short rectangular strait for six different heating rates. Total depth is 7 cm.

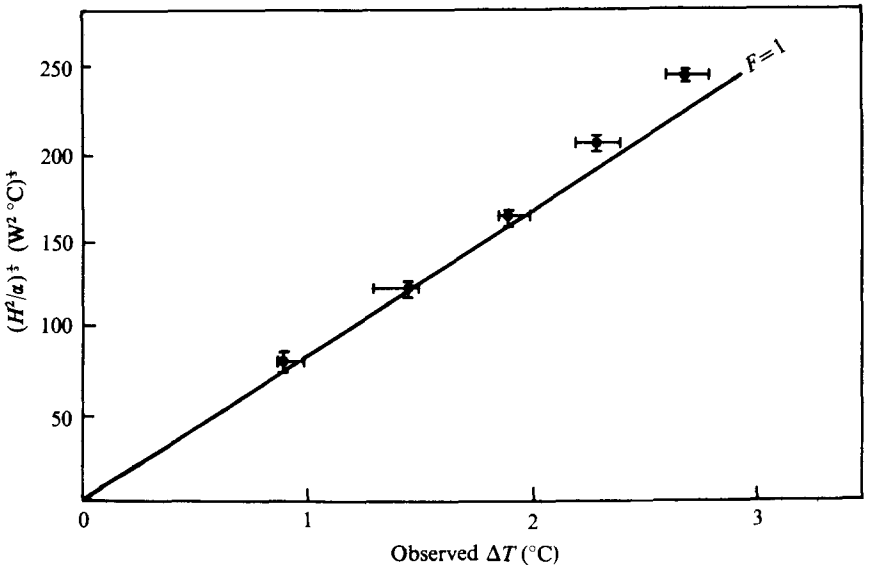

FIGURE 4. Comparison of six measurements (constant depth) with the computed line for critical Froude conditions.

was covered and the walls insulated. Temperatures were measured with a thermistor, at vertical spacings of 0·5 cm.

Visualization by aluminium powder showed that a steady two-layer current was consistently established, with the interface sloping down towards the heated basin (figure 2, plate 1). Because of this slope, it is relevant to specify where each measurement was taken. Six measurements were taken for each profile: three at the cold end and three at the warm end of the strait. Figure 3 shows these two groups for each heating rate H.

The value of α was calculated separately for each case because its variation with temperature is not negligible. The temperature difference ΔT (between the upper and the lower layer) compares well with the theoretical ΔT computed for critical interfacial Froude conditions, as indicated in each profile by the horizontal dashed segment in figure 3.

Equation (1.10) predicts a linear relation between ΔT and $(H^2/\alpha)^{\frac{1}{3}}$ for any fixed

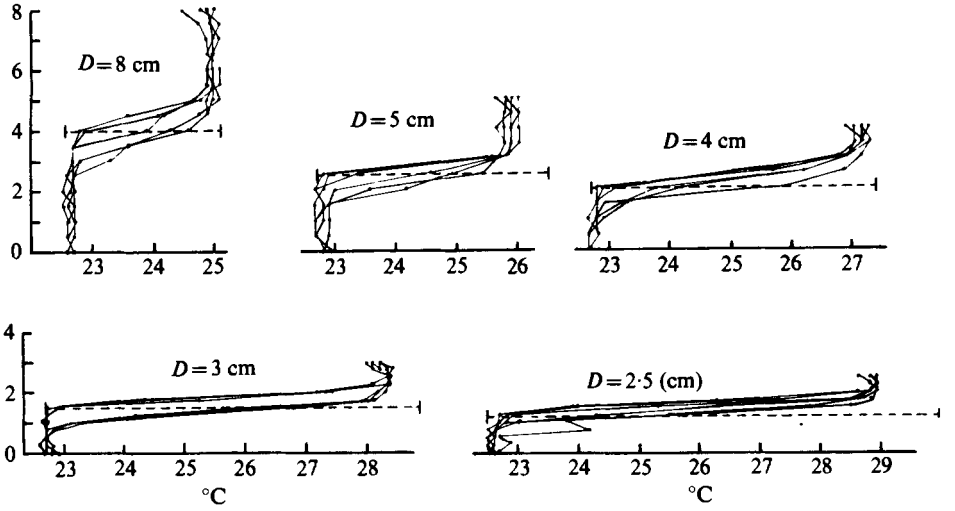

FIGURE 5. Temperature profiles in the short rectangular strait for five different depths. Heating rate is 53·5 W.

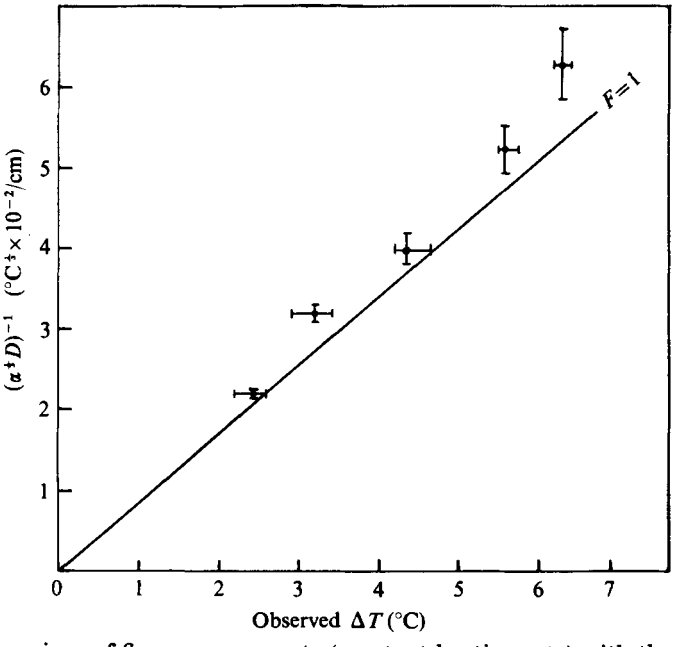

FIGURE 6. Comparison of five measurements (constant heating rate) with the computed line for critical Froude conditions.

depth. The measurements and the predicted ($F = 1$) line for $D = 7$ cm are plotted in figure 4. Except for some heat loss at the higher heating rates, the fit appears to be within the accuracy of the experiment.

In a second experiment, the heating rate was fixed at $H = 53{\cdot}5$ W while the depth D was varied from 8 cm down to 2·5 cm. The profiles are shown in figure 5. Equation (1.12) predicts a thermocline thickness of about $\frac{1}{5}$. At the smallest depth, the vertical

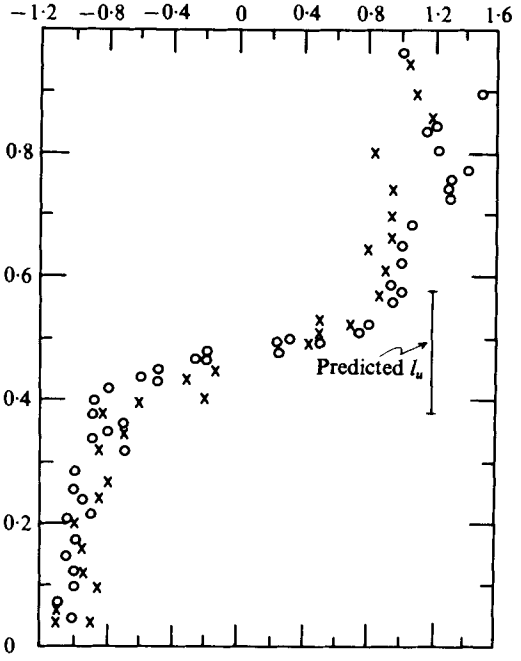

FIGURE 7. Velocity profile in the short rectangular strait (relative length of streaks *vs.* relative vertical distance from sill).

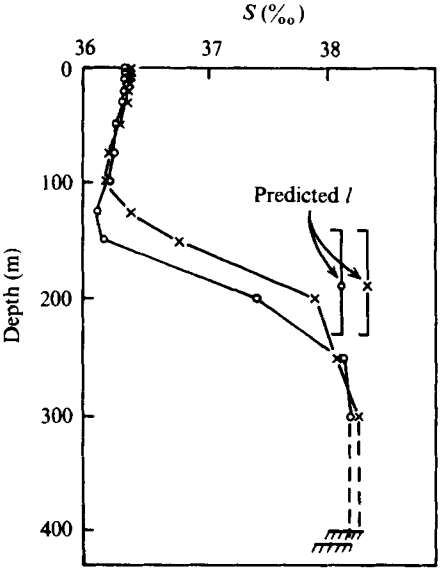

FIGURE 8. Salinity profiles in the Strait of Gibraltar. ○, standard depth averages of Calypso stations 563–584 (May 1961); ×, standard depth averages of Calypso stations 702–724 (June 1961).

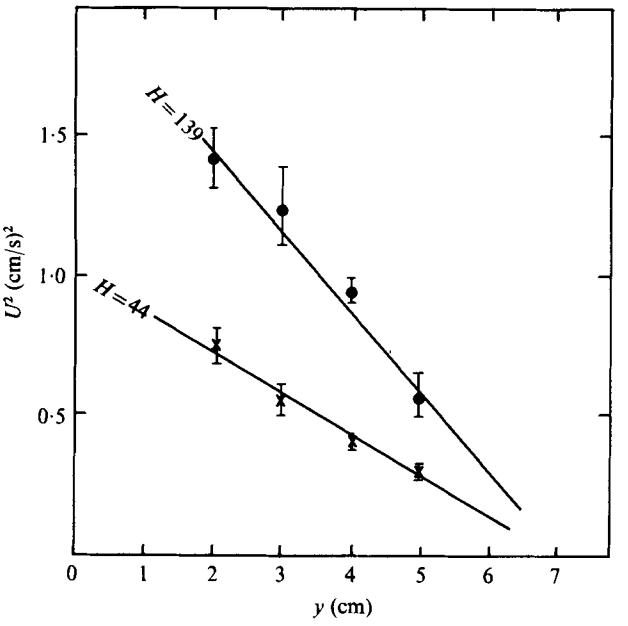

FIGURE 9. Square of velocity of particles *vs.* distance from wall. Triangular cross-section, lower layer.

spacing of the measurements did not allow accurate determination of the thermocline thickness, however the general trend seems adequate. Here again there is apparently some heat loss, but measurements lie reasonably close to the theoretical line in figure 6.

The relative interlayer thickness l/D was determined graphically for the five runs with constant H and the six runs with constant D, and found to give a mean of 0·20 with a standard deviation of 0·02, in good accordance with (1.12).

Before (2.1), we argued that the shear thickness l_u should be the same as the thermocline thickness l. By measuring the lengths of the streaks made by the aluminium particles, a graph of relative speed versus relative depth was constructed (figure 7). The predicted thickness is also shown in the figure, and the fit appears satisfactory. With this support to our Richardson number argument, we tried to apply it to a short ocean strait. The Strait of Gibraltar is about 60 km long and 350 m deep, and therefore, according to (1.13), should be moderately short. Standard depth data from Calypso stations 563–584 and 707–724 were taken from an NODC tape and are plotted in figure 8, along with the predicted halocline thickness. The fit seem well within 'oceanographic accuracy'.

4. Canted short-strait experiments

In order not to be confined to rectangular straits, we performed some experiments with a triangular notch in the separating wall (figure 1*b*). The deepest part was 5·6 cm, and the width at the water-line was 10·5 cm. The general behaviour appeared to be similar to that of the rectangular strait. The basic postulate was that the flow in short straits should be such that $F = 1$. A natural strait is likely to be much wider than it is deep, so we may well expect this criterion to hold locally. Our strait is rather narrow, but nonetheless warrants inspection.

If the upper and lower layers were to have equal speeds, their cross-sectional areas would be equal, and the lower layer ought to reach $y = 10{\cdot}5/\sqrt{2} = 7{\cdot}1$ cm. The depth D_2 should increase linearly to the edge and one would expect a constant value of $U^2/g'D_2$. Figure 9 shows a plot of U^2 *vs.* y for two runs, with straight lines fitted through $y = 7{\cdot}1$ cm. The flow in the outer centimetre, closest to the outside wall, appeared to be affected by heat loss and side friction, and therefore is not plotted; otherwise the straight lines seem to fit quite reasonably, and do support the idea of a constant Froude number. Substitution of the rather rough measurements of ΔT, D_1, D_2 and U gives values for (1.1) which are closer to 1·3 than to 1·0.

Measurements for the thermocline thickness showed that it did increase at the deeper end, but not as fast as the total depth.

5. Long-strait experiment

A channel 1 cm wide, 7·75 cm deep and 60 cm long was placed as shown in figure 1 (*c*). The inner walls of the channel and its bottom were insulated to minimize heat losses. A heating rate of 50 W was supplied by the heater, and the temperatures were measured along 11 profiles, at vertical spacings of 0·5 cm, as shown in figure 10. The whole set of measurements was repeated after about 20 min (the time required to complete a whole run) and the profiles showed good reproducibility (figure 10*a*), indicating that a steady state was reached.

The height of zero speed was determined from the flow visualization, and is marked by the arrows in figure 10 (*a*). This height is displaced towards the slower moving side from the height of maximum shear.

The temperature in each layer is uniform, and the thermocline well defined. Its shape (figure 10*b*) of an essentially linear interior with sharp curves at the ends is much like the solutions of Assaf & Hecht (1974). Graphically we find l to be about 0·14, or one-seventh of the total depth. Therefore we find the thermocline in a long strait to be sharper than the thermocline in a short strait, in accordance with our remark in § 2.

Equation (2.11) predicts the change in depth between the two ends. Substituting for the chosen constants, we have

$$\beta = 2{\cdot}64(1-\beta^2)^2(1+3\beta^2)^{-\frac{3}{2}}, \tag{5.1}$$

which gives $\beta = 0{\cdot}615$. We do not know the precise profile, but a straight line, as suggested by Assaf & Hecht (1974) for the interior, should be a good approximation. A heavy line through the centre with a slope of $\beta = 0{\cdot}615$ is shown in figure 10 (*b*). The centre of the observed thermocline is lower, but the predicted slope agrees fairly well.

The long-strait theory presented in § 2 depends on the assumption (2.3) that $F = 1$ at the ends, while $F < 1$ in the interior. The observed Froude number F, plotted against horizontal distance in figure 10 (*c*), verifies this point; as expected, the Froude number is low in the interior and increases to unity at each end.

6. Conclusion

A great deal of the behaviour of straits can be explained simply by Froude and Richardson number arguments. The validity of this approach is evident from the fact that it is applicable to straits covering wide ranges of size and buoyancy flux, from natural ones to laboratory mini-straits.

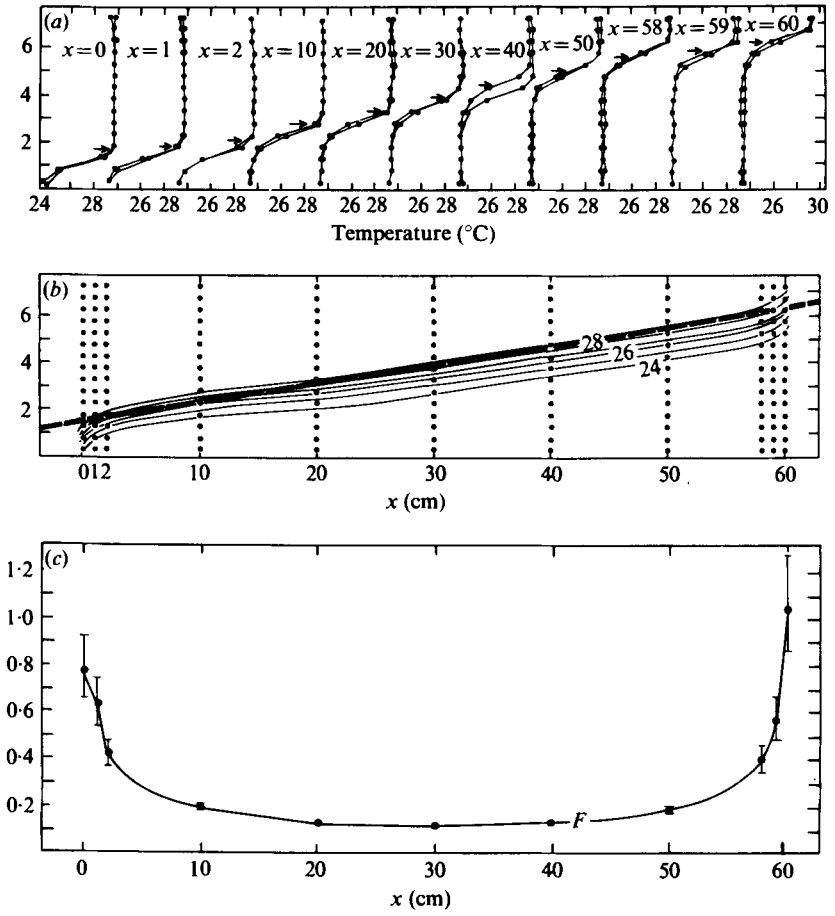

FIGURE 10. Measurements in the long strait. Heating rate is 50 W. Depth is 7·75 cm. (*a*) Temperature profiles at 11 distances along the length of the strait. Arrows denote the height of zero speed. (*b*) A longitudinal temperature section along the strait. The abscissa x is the distance from the warmed basin. The heavy dashed line, with slope $\beta = 0{\cdot}615$, is the solution of (5.1). (*c*) The measured F at 11 distances along the length of the strait.

A criterion has been suggested for identifying dynamically short straits. On this basis, the Bosphorus, Bab-el-Mandeb and the Dardanelles are long straits, the Strait of Gibraltar is marginal, while the Strait of Tiran is a short strait.

Evidence has been presented which indicates that in a strait of variable depth there is a tendency for locally critical flow.

Thanks are due to U. Siegenthaler for his close cooperation during the early stages of this work and for reviewing the manuscript. This research was supported by a grant from the United States–Israel Binational Science Foundation (BSF), Jerusalem, Israel.

REFERENCES

ASSAF, G. & HECHT, A. 1974 Sea straits: a dynamical model. *Deep-Sea Res.* **21**, 947–958.

BUSINGER, J. A., WYNGAARD, J. C., IZUMI, Y. & BRADLEY, E. F. 1971 Flux profile relationships in the atmospheric surface layer. *J. Atmos. Sci.* **28**, 181–189.

DEFANT, A. 1961 *Physical Oceanography*, vol. 1. Pergamon.

MELLOR, G. L. 1973 Analytic prediction of the properties of stratified planetary surface layers *J. Atmos. Sci.* **30**, 1061–1069.

STOMMEL, H. & FARMER, G. H. 1953 Control of salinity in an estuary by a transition *J. Mar. Res.* **12**, 13–20.

WEBB, E. K. 1970 Profile relationships: the log–linear range and extension to strong stability *Quart. J. Roy. Met. Soc.* **96**, 67–90.

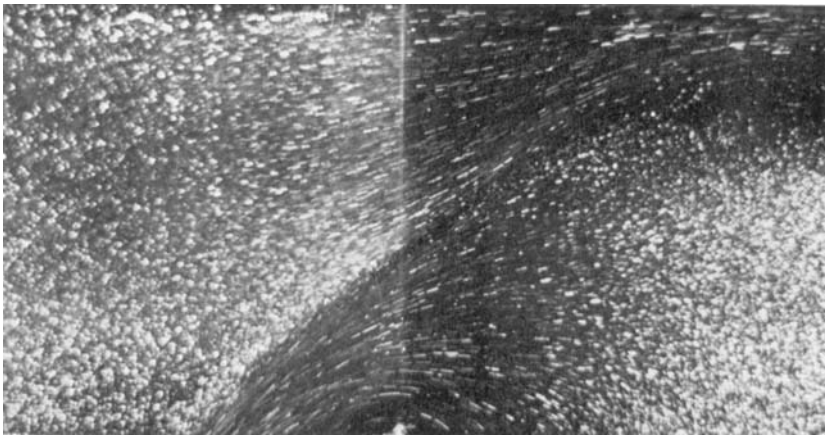

FIGURE 2. Two-layer flow through a short rectangular strait. Side view, $\frac{1}{4}$ s exposure.